Journal of Nuclear Energy Parts A/B, 1965, Vol. 19, pp. 527 to 539. Pergamon Press Ltd. Printed in Northern Ireland

A CALORIMETRIC DETERMINATION OF FISSION PRODUCT HEATING IN FAST REACTOR PLUTONIUM FUEL

K. JOHNSTON
Atomic Weapons Research Establishment, Aldermaston, Berks.

(*Received* 10 *December* 1964)

Abstract—Fission product heating in plutonium irradiated in the Dounreay Fast Reactor has been measured using a Calvet microcalorimeter. By use of small, lightly canned samples and a γ-absorber, the β- and γ-power contributions were measured separately over a range of decay times between 40 and 150 days after shutdown.

1. INTRODUCTION

FROM the nuclear standpoint, ^{239}Pu is an attractive fuel for fast reactors and much current work is being devoted to the development of suitable nuclear fuels based on plutonium.

An important aspect of the technology of any nuclear fuel is the energy produced by the decay of the radioactive fission products. After discharge from the reactor, fuel rods are stored while ^{131}I decays and are then transported to the chemical reprocessing plant for recovery of residual fissile materials. Provision of adequate cooling for irradiated fuel elements during storage and transit depends on an accurate knowledge of the fission product heat output.

As a result of extensive theoretical summation studies and experimental measurements, the fission product heat output from slow neutron irradiated ^{235}U is now well-characterized. This work is usefully summarized in the papers of PERKINS and KING (1958) and STEHN and CLANCY (1958). However, the lack of fission product yield data for fast-fissioned ^{239}Pu has precluded summation studies; moreover, no direct experimental measurements have been reported.

The present paper describes a calorimetric determination of fission product heating in plutonium fuel irradiated in the Dounreay Fast Reactor (D.F.R.). Experimental results have been fitted to empirical equations of the type derived by WAY and WIGNER (1948) and related to the number of fission events by radiochemical analysis.

2. EXPERIMENTAL

2.1 *Sample preparation*

Each sample consisted of 40 mg of powdered PuO_2 which was accurately weighed and doubly-sealed in thin-walled aluminium capsules as shown in Fig. 1. The outer capsule, which contained an atmosphere of helium, was sealed by arc welding and carried a drilled tag for suspension during calorimetric measurements.

To ensure maintenance of sample integrity during irradiation in the D.F.R. core,

each aluminium capsule was sealed into a section of stainless-steel tube in an atmosphere of helium. These steel capsules were leak-tested, incorporated into niobium fuel pieces and finally loaded into D.F.R. Mk. II fuel elements.

Samples of the PuO_2 used to fill the irradiation capsules were analysed chemically to check the purity and stoichiometry of the oxide, and mass spectrometrically to determine the proportions of the minor constituent isotopes ^{240}Pu and ^{241}Pu. The small proportion of ^{241}Am present as a consequence of decay of ^{241}Pu was determined by anion exchange separation followed by α-counting.

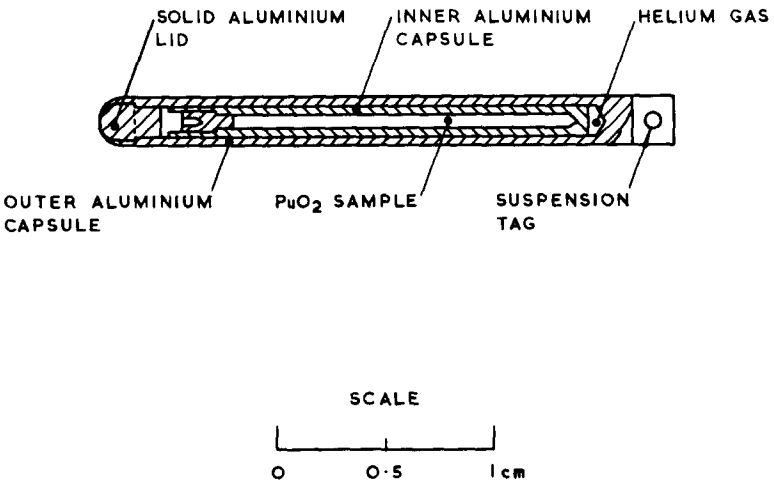

FIG. 1.—Sample capsule.

2.2 *Irradiations*

A total of four PuO_2 samples plus two 'blanks' (containing empty aluminium capsules) were loaded into the D.F.R. core. Samples 1 and 2 plus one blank were loaded into the same niobium fuel piece near the core centre, while samples 3 and 4 and the second blank were also loaded together, but in a channel nearer the edge of the core in a region of lower neutron flux.

Because of the experimental programme of the Fast Reactor, samples were irradiated intermittently, as shown in Fig. 2. Samples 1 and 2 received a four-part irradiation to a total integrated flux of $1{\cdot}88 \times 10^{21}$ n cm^{-2} while samples 3 and 4 required six irradiations to achieve an integrated flux of $1{\cdot}89 \times 10^{21}$ n cm^{-2}. These neutron exposures were calculated from the measured thermal ratings of the reactor and the computed flux distribution across the core.

2.3 *Calorimetry*

Calorimetric measurements were carried out with a microcalorimeter of the type described by CALVET and PRAT (1956). The calorimeter consists of two thin-walled cylindrical silver cells set in cavities in a thermostatically controlled aluminium block, but separated from it by gaps spanned by multiple-junction thermopiles, the interstices being filled with a low-density thermal insulator. The cells and aluminium blocks are contained in a multi-walled thermostat enclosure as shown in Fig. 3.

The sample is inserted into one of the cells and the temperature difference between

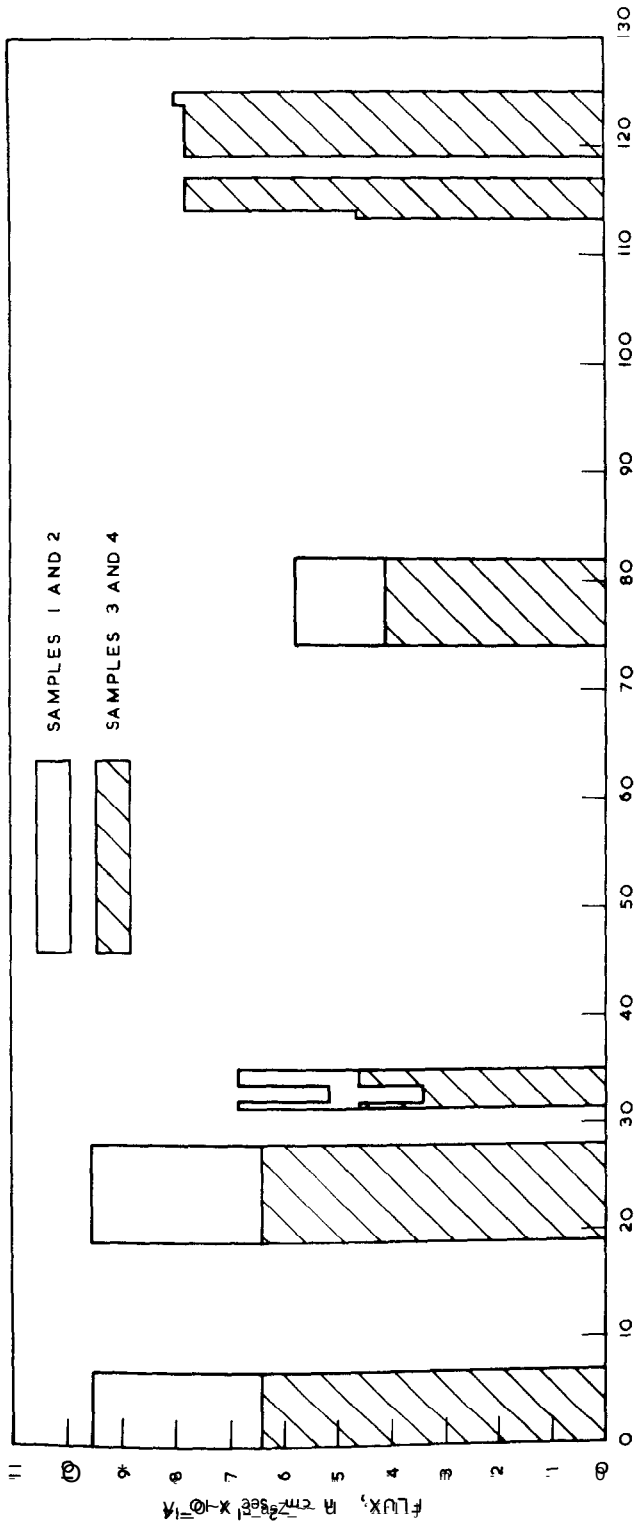

FIG. 2.—Sample irradiations in D.F.R.

the cells is monitored by a differential thermopile, the output of which is fed to a spot galvanometer and displayed on a chart by the pen of a spot-follower. By passing current through a subsidiary bank of thermocouples, heat can be 'pumped' out of the sample cavity at a controlled rate, using the Peltier effect. Thus, by adjusting the

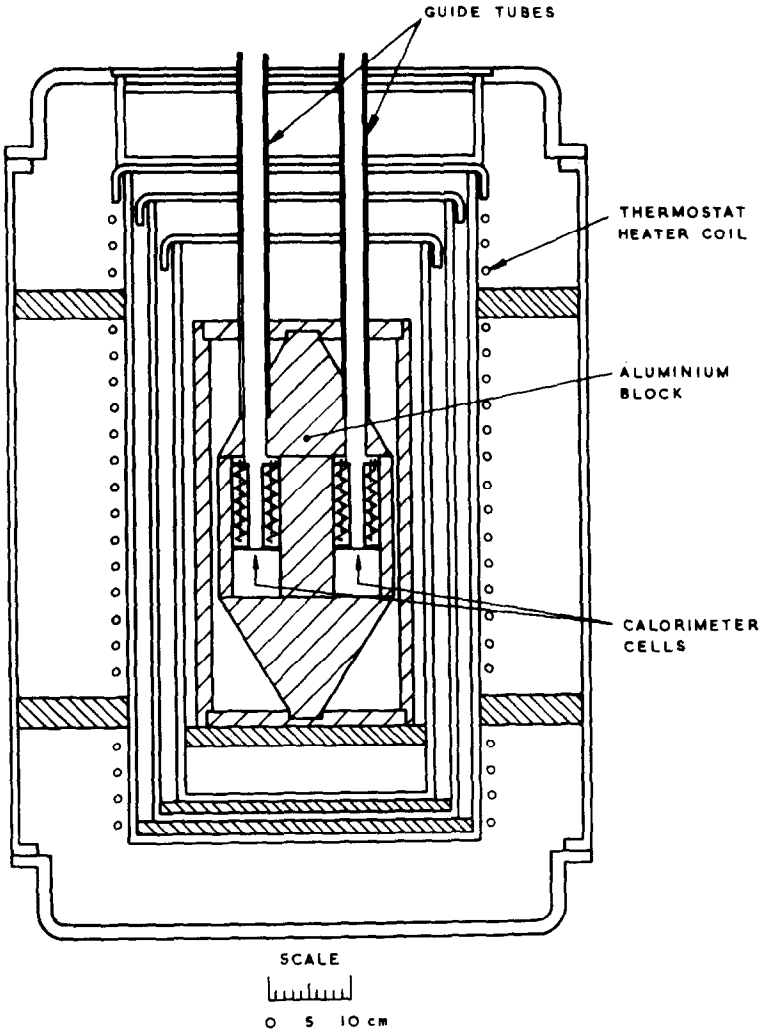

FIG. 3.—General view of microcalorimeter.

known rate of Peltier cooling so as to cancel the heat output of the sample, the temperature difference between the cells is reduced to zero.

In the present determinations, the radioactive samples were measured with and without a cylindrical uranium γ-absorber. Figure 4(a) shows the absorber lowered to surround the sample and absorb a high proportion of the emitted γ-rays, while Fig. 4(b) shows the absorber raised, leaving the sample freely suspended within the sample cavity. In both positions, loss of heat from the cavity to the vertical guide tubes is prevented by the insulating 'Tufnol' end-pieces of the uranium absorber which seal the opening of the sample cell. An identical absorber was manufactured to fit the

reference cell of the calorimeter, sample and absorbers being raised and lowered independently by suspension threads attached to a lifting device at the deck of the calorimeter.

The system was calibrated electrically by means of a heater wound on a cylindrical former of the same size as the sample capsule, and the calibration was checked by

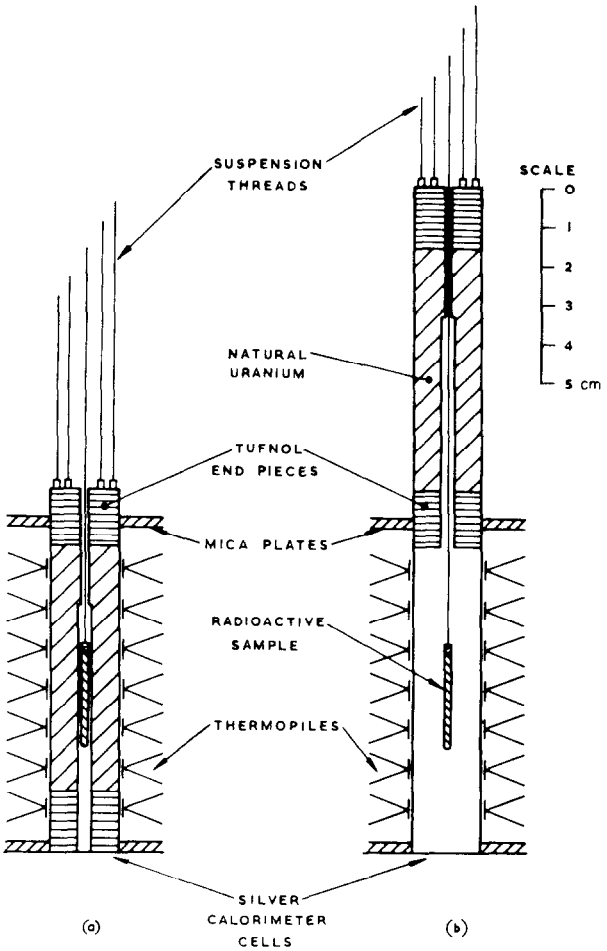

FIG. 4.—Positioning of uranium absorber during calorimetric measurements.

measurement of a standard radium needle of similar physical dimensions. This revealed that, provided the sample was always suspended at the same height within the sample cavity, the sensitivity of the calorimeter was the same whether measurements were made with the uranium absorber raised or lowered. The calibration was accurate to better than ± 1 per cent.

2.4 *Gamma absorption measurements*

The relative intensities of the γ-energy peaks emitted by the irradiated samples were measured at intervals using a sodium iodide crystal spectrometer. At decay times

greater than 40 days after shutdown, virtually all the γ-energy was emitted in the peaks at 0·50, 0·77 and 1·60 MeV.

The absorption of these γ-energy peaks by the uranium absorber was measured with the same crystal spectrometer. Peak intensities escaping from the thin-walled aluminium sample capsule were measured for rays making various angles with the axis of the cylindrical sample. Then, with the sample sheathed by the cylindrical uranium absorber, the diminution of peak intensities was measured at the same angular settings. Polar diagrams of the γ-peak intensities escaping from the absorber were thus obtained, and these were integrated to yield the percentage γ-energy absorbed for each peak.

These absorption factors were then applied to the γ-spectra measured at various decay times in the range 40–150 days after shutdown, giving the percentage of the total fission product γ-power dissipated in the absorber as a function of time after shutdown.

2.5 *Fission product analysis*

While calorimetric measurements with samples 2, 3 and 4 were in progress, sample 1 was dissolved for radiochemical analysis of ^{90}Sr, ^{95}Zr and ^{144}Ce and for mass spectrometric analysis of plutonium. The half-lives of the nuclides measured were sufficiently long to enable them to reflect fissions occurring at the beginning of the irradiation period; moreover, their fission yields lay on the peaks of the mass–yield curve and were therefore relatively insensitive to small changes in the energy spectrum of the neutrons inducing fission.

Radiochemical analysis gave the number of fissions occurring in sample 1 as $2{\cdot}66 \times 10^{17}$, $2{\cdot}73 \times 10^{17}$ and $2{\cdot}61 \times 10^{17}$ as derived from the results obtained for ^{90}Sr ^{95}Zr and ^{144}Ce respectively. This gave an average result of $2{\cdot}67 \times 10^{17}$ fissions, which is considered accurate to $\pm 3\%$.

By replicate mass-spectrometric measurements of solution aliquots which had been 'spiked' with known quantities of ^{242}Pu, it was determined that sample 1 contained $8{\cdot}19 \times 10^{19}$ atoms of plutonium, of which 96·38% was ^{239}Pu. Since sample 1 was exposed to an integrated flux of $1{\cdot}88 \times 10^{21}$ n cm^{-2}, this indicated that the 'average' fission cross section of plutonium of this particular composition in the D.F.R. was 1·73 barns. Alternatively, by assuming fission cross sections of 1·3 and 1·1 barns for ^{240}Pu and ^{241}Pu which contributed respectively $2{\cdot}84 \times 10^{18}$ and $1{\cdot}3 \times 10^{17}$ atoms to the total quoted above, the ^{239}Pu fission cross section was derived as 1·75 barns for the D.F.R. neutron spectrum.

3. RESULTS

Calorimetric measurements were made over a period of about 100 days for sample 2 and 70 days for samples 3 and 4. Heat outputs measured experimentally are listed in Table 1. The symbol H_A denotes the heat output measured with the uranium absorber surrounding the sample, while H_0 is the heat output measured with absorber raised. The difference $(H_A - H_0)$ is also listed as this is useful in deriving H_γ, the fission product γ-power.

Since measurement of the 'blank' capsules showed that no detectable heat output could be ascribed to activation occurring in the aluminium capsules, the heat outputs

TABLE 1

Sample	Shutdown time (d)	$H_0(\mu W)$	$H_A(\mu W)$	$(H_A - H_0)(\mu W)$
2	46	389·5	634·9	245·4
	67	314·7	487·6	172·9
	76	295·3	444·1	148·8
	90	271·2	401·5	130·3
	110	242·8	346·6	103·8
	144	214·2	285·5	71·3
3	54	339·3	525·8	186·5
	62	312·2	473·0	160·8
	75	280·0	409·8	129·8
	97	242·6	340·8	98·2
	125	218·6	295·2	76·6
4	53	345·1	552·6	207·5
	61	331·8	505·2	173·4
	74	294·7	436·7	142·0
	96	261·9	364·4	102·5
	124	228·5	313·1	84·6

measured experimentally could be expressed as summations of contributing factors as follows:

$$H_0 = H_\beta + H_\gamma^S + H_{0\gamma}{}^I + H_{\mathrm{Pu}} + H_{\mathrm{CAP}} \tag{1}$$

$$H_A = H_\beta + H_\gamma^S + H_{A\gamma}{}^I + H_{\mathrm{Pu}} + H_{\mathrm{CAP}} + H_\gamma{}^{\mathrm{U}} \tag{2}$$

and

$$H_A - H_0 = H_\gamma{}^{\mathrm{U}} + H_{A\gamma}{}^I - H_{0\gamma}{}^I, \tag{3}$$

where

H_β = fission product β-power
H_γ^S = fission product γ-power absorbed in sample capsule
$H_\gamma{}^{\mathrm{U}}$ = fission product γ-power absorbed in uranium absorber when lowered to surround the sample
$H_{0\gamma}{}^I$ = measured power output due to γ-absorption in the calorimeter cell wall and insulator–thermopile block (with absorber raised)
$H_{A\gamma}{}^I$ = measured power output due to γ-absorption in the calorimeter cell wall and insulator–thermopile block (with absorber lowered)
H_{Pu} = α-decay power due to unfissioned plutonium

and

H_{CAP} = decay power output of capture products.

These contributions to the measured heat outputs are now considered in sequence.

H_β: Even with the absorber raised, the sample capsule, air gap and silver cell wall constitute an absorber of thickness 834 mg cm^{-2}. This is sufficient to absorb more than 99·9 per cent of the emitted β-energy. Thus H_β appears unmodified in equations (1) and (2).

H_γ^S: The γ-energy absorbed within the sample capsule was calculated by treating the sample as a line emitter and applying end-absorption corrections derived from the angular γ-intensity measurements described in Section 2.4. This gave the result that

2·0 per cent of the fission product γ-power was absorbed in the capsule, and that this proportion did not vary significantly during the measurement period. That is

$$H_\gamma^S = 0{\cdot}020\ H_\gamma.$$

H_γ^U: The absorption of γ-energy in the uranium cylinder was measured at intervals as described in Section 2.4. Results are displayed in Fig. 5, slight differences between

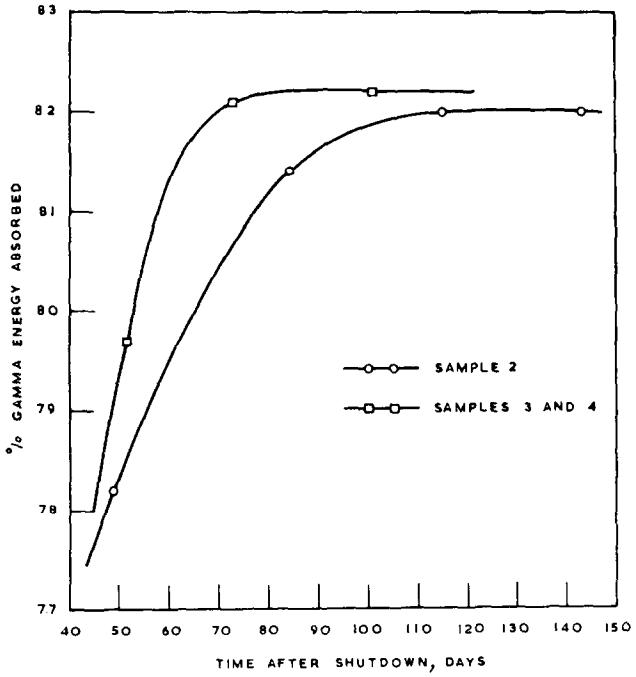

FIG. 5.—Percentage absorption of emitted gross γ-energy by the uranium absorber, measured as a function of time after shutdown.

results for sample 2 and samples 3 and 4 being due to the different irradiation histories of the samples. By using the data from Fig. 5, H_γ^U could be expressed as a fraction of H_γ at any time after shutdown (bearing in mind that only 0·98 H_γ escaped from the encapsulated sample).

$H_{0\gamma}^I$ and $H_{A\gamma}^I$: Whether the sample was suspended freely within the sample cavity or sheated by the uranium absorber, γ-energy escaping from the sample cavity was partially absorbed in the thin silver cell wall and the insulator–thermopile block.

Simple calculation showed that 1·5 per cent of the incident γ-energy was absorbed in the silver cell wall. However, the effect caused by γ-energy dissipated throughout the complex array of thermocouple wires and low-density insulator was more difficult to estimate. By assuming the block to be of uniform density, theoretical analysis of the heat flows set up by γ-absorption within the block (based on the measured thermal conductivity) showed that the effect was *as if* 3·5 per cent of the incident γ-energy had been deposited within the sample cell.

Thus, summing the effects, $H_{0\gamma}^I$ and $H_{A\gamma}^I$ were calculated by assuming them to amount to 5 per cent of the incident γ-power. This proportion was taken as constant for the minor spectral changes occurring during the measurement period.

H_{Pu}: The heat outputs of the fuel samples themselves were measured prior to irradiation. The results were in good agreement with heat outputs calculated from weights of oxide and the analytical data.

By allowing for burn-up of ^{239}Pu during irradiation and growth of ^{241}Am activity due to decay of ^{241}Pu, values of H_{Pu} of 80·6, 80·7 and 83·4 μW were obtained for samples 2, 3 and 4 respectively.

TABLE 2

Sample	Time (d)	$H_\gamma{}^S$	$H_{A\gamma}{}^I$	$H_{0\gamma}{}^I$	H_{Pu}	$H_\gamma{}^U$	H_β	H_γ	$H_{\beta+\gamma}$
2	46	6·8	3·7	16·6	80·6	258	286	339	625
	67	4·6	2·2	11·3	80·6	182	218	232	450
	76	4·0	1·9	9·7	80·6	157	201	198	399
	90	3·4	1·6	8·4	80·6	137	179	172	351
	110	2·7	1·2	6·7	80·6	109	153	136	289
	144	1·9	0·8	4·6	80·6	75	127	94	221
3	54	5·0	2·5	12·3	80·7	196	241	250	491
	62	4·2	1·9	10·4	80·7	169	217	212	429
	75	3·4	1·5	8·3	80·7	137	188	170	358
	97	2·6	1·1	6·3	80·7	103	153	128	281
	125	2·0	0·9	4·9	80·7	81	131	100	231
4	53	5·6	2·7	13·7	83·4	218	243	278	521
	61	4·6	2·1	11·2	83·4	183	233	229	462
	74	3·7	1·6	9·1	83·4	150	199	186	385
	96	2·7	1·2	6·6	83·4	108	169	134	303
	124	2·2	1·0	5·4	83·4	89	137	111	248

H_{CAP}: Comparison of pre-irradiation and post-irradiation mass spectrometric analyses showed that the ratio $^{240}Pu/^{239}Pu$ had increased from 0·0352 to 0·0360 during irradiation. This implied that for any of the samples H_{CAP} was less than 0·5 μW. Consequently, H_{CAP} was neglected in the present study.

By evaluating the contributing heat outputs enumerated above for each experimental measurement listed in Table 1, it was possible from equations (1)–(3) to calculate the corresponding values of H_β and H_γ. Results thus obtained are displayed in Table 2, together with the contributing heat outputs used in the derivation. As before, all heat outputs are in μW.

By considering the possible errors in the above derivation, together with a maximum error ± 1 per cent in the calorimetric measurements, it was possible to derive the following 95 per cent confidence limits, H_β: $\pm 4\%$, H_γ: $\pm 7\%$ and $H_{\beta+\gamma}$: $\pm 3\%$. The relatively high error in H_γ is due to possible experimental inaccuracies of about 4 per cent in the γ-absorption measurements, while the low error in $H_{\beta+\gamma}$ is due to the fact that the values of H_β and H_γ are not independent but are linked by equations (1)–(3). Because of this interdependence, some individual errors in H_β and H_γ are halved when considering their sum, while others cancel when summed to give $H_{\beta+\gamma}$ since they are of equal magnitude, but opposite sign.

The results shown in Table 2 represent the fission product decay heating following intermittent irradiations at various flux ratings. Derivation of more useful relationships was carried out by representing the decay heating $H(t)$ due to each increment of irradiation by an equation of the form

$$H(t) = SN\sigma f[t^{-x} - (t + T)^{-x}] \text{ W}$$

where

S = a constant

N = total number of plutonium atoms

σ = average fission cross section for plutonium (cm^2)

f = average neutron flux during irradiation (n $cm^{-2}sec^{-1}$)

T = irradiation time (days)

t = decay time (days).

By fitting the summation of such decays to the experimental results it was possible, from the known irradiation data and derived fission cross section, to obtain the best values of the decay exponent x and the constant S for each decay heat output. The

TABLE 3

MeV/sec fission	W/fission	W/M.W.D.
$H_{\beta+\gamma}$ $4{\cdot}07 \times 10^{-6} t^{-1{\cdot}29}$	$6{\cdot}52 \times 10^{-19} t^{-1{\cdot}29}$	$1{\cdot}77 \times 10^{3} t^{-1{\cdot}29}$
H_{γ} $5{\cdot}86 \times 10^{-6} t^{-1{\cdot}53}$	$9{\cdot}39 \times 10^{-19} t^{-1{\cdot}53}$	$2{\cdot}55 \times 10^{3} t^{-1{\cdot}53}$
H_{β} $0{\cdot}741 \times 10^{-6} t^{-1{\cdot}06}$	$1{\cdot}18 \times 10^{-19} t^{-1{\cdot}06}$	$0{\cdot}320 \times 10^{3} t^{-1{\cdot}06}$

equations derived in this manner for $H_{\beta+\gamma}$ and H_{γ} for all three samples were in excellent agreement. However, because of the slower decay rate of H_{β}, small measurement errors became relatively more significant and the results for H_{β} showed rather poorer correspondence. By averaging the results for samples 2, 3 and 4, the following best equations were obtained:

$$H_{\beta+\gamma} = 1{\cdot}94 \times 10^{-13} N \sigma f [t^{-0{\cdot}29} - (t + T)^{-0{\cdot}29}] \text{ W} \quad (4)$$

$$H_{\gamma} = 1{\cdot}53 \times 10^{-13} N \sigma f [t^{-0{\cdot}53} - (t + T)^{-0{\cdot}53}] \text{ W} \quad (5)$$

$$H_{\beta} = 1{\cdot}71 \times 10^{-13} N \sigma f [t^{-0{\cdot}06} - (t + T)^{-0{\cdot}06}] \text{ W} \quad (6)$$

Heat outputs computed using the above equations are subject not only to the errors listed above as applicable to the derived values of $H_{\beta+\gamma}$, H_{γ} and H_{β}, but also to the uncertainty of about $\pm 3\%$ incurred in estimating the number of fissions occurring in each sample. Thus, heat outputs derived from equation (4) have 95% confidence limits of about $\pm 6\%$, those from equation (5) $\pm 10\%$, and those from equation (6) $\pm 7\%$.

Equations (4)–(6) permit derivation of the decay powers following an instantaneous 'burst' of fissions. Results are shown in Table 3. The first two columns show the decay powers expressed in MeV/sec fission and W/fission, these expressions being derived directly from equations (4)–(6) by use of the average cross section of 1·73 barns derived in Section 2.5. However, the additional factor of 199 MeV/fission was employed to derive the 'W/M.W.D.' data shown in the third column. The value of 199 MeV/fission denotes the prompt energy liberated in fast fission of ^{239}Pu and compares with about 186 MeV/fission for slow-fissioned ^{235}U.

4. DISCUSSION

Since equations (4)–(6) represent the best fit to the experimental data, they apply strictly only to the range of irradiation and decay times covered by the measurements.

In particular, no sample was irradiated continuously for more than 9 days, although total exposures reached as high as 37 days. Thus, the use of these equations to calculate fission product heating after prolonged irradiations (300 days for an economic fast reactor) is not a valid procedure. As fission yield data for fast-fissioned ^{239}Pu become available, the extension of the validity of the present measurements by theoretical summation studies should be possible.

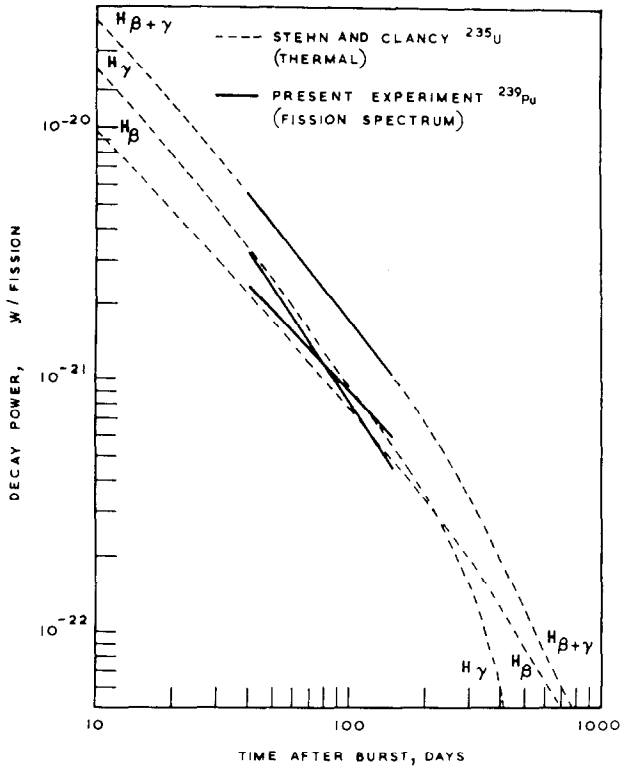

FIG. 6.—Fission product decay power following an instantaneous burst of fissions.

In the absence of such summation studies, comparison of the present results with the fission product decay heating in slow-fissioned ^{235}U is instructive. For convenience, comparison is made with the data of STEHN and CLANCY since these cover the same range of decay times and are, moreover, consistent with the calorimetric measurements of DAY and CANNON (1951). Because of the short irradiations used in the present work, comparison is made between results derived for decay heating following an instantaneous 'burst' of fissions (Table 3).

Figure 6 shows the correspondence of the two sets of data when expressed in terms of W/fission. The agreement between the results for $H_{\beta+\gamma}$ is most striking. The agreement between the pairs of curves for H_β and H_γ is not so close, but the discrepancies seldom exceed 15 per cent and are thus probably within the limits of error for the two sets of data.

Results are also compared in Fig. 7 using the more 'practical' units of W/M.W.D. This shows that the fast reactor operator using ^{239}Pu obtains the same thermal power

output with the production of about 6 per cent less residual fission products in the spent fuel. This is a direct consequence of the fact that fast fission of ^{239}Pu is more energetic than slow neutron fission of ^{235}U.

In conclusion, it is clear that, when related to fission events, gross fission product

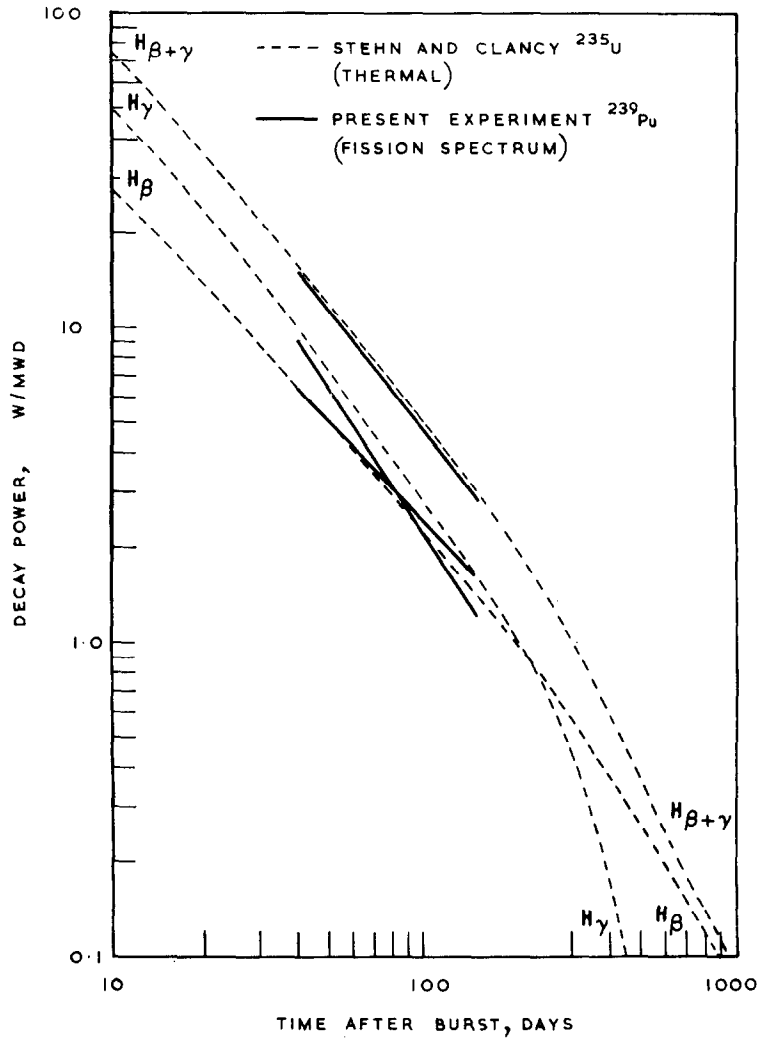

FIG. 7.—Fission product decay power following an instantaneous burst of fissions.

decay heating in fast-fissioned ^{239}Pu is closely similar to that of slow-fissioned ^{235}U. However, the pattern of build-up of capture products in the two fuels as irradiation proceeds will be quite different, and different allowances will have to be made for capture product heating.

Acknowledgments—The author is glad to acknowledge the advice and co-operation of Dr. A. G. EDWARDS and Mr. J. C. W. TELFER of the Fast Reactor Physics Group, Dounreay. Thanks are also due to Mr. D. G. VALLIS, AWRE for the determination of the number of fission events as derived from the radiochemical measurements.

REFERENCES

CALVET E. and PRAT H. (1956) *Microcalorimétrie* Masson et Cie, Paris.
DAY R. A. and CANNON C. V. (1951) Radiochemical Studies: *The Fission Products*, Paper 41, *National Nuclear Energy*, Series IV, Vol. 9, p. 422, McGraw-Hill, New York.
PERKINS J. F. and KING R. W. (1958) *Nucl. Sci. Engng.* **3,** 726.
STEHN J. R. and CLANCY E. F. (1958) *Proceedings of the Second International Conference on the Peaceful Uses of Atomic Energy, Geneva*, A/Conf. 15/P/1071. United Nations, N.Y.
WAY K. and WIGNER E. P. (1948) *Phys. Rev.* **73,** 1318.